Science of the Total Environment 704 (2020) 135928

Contents lists available at ScienceDirect

Science of the Total Environment

journal homepage: www.elsevier.com/locate/scitotenv

Study of mercury transport and transformation in mangrove forests using stable mercury isotopes

Shuyuan Huang [a], Ronggen Jiang [a], Qingyong Song [b], Yuanbiao Zhang [a,*], Qi Huang [c], Binghuan Su [c], Yaojin Chen [b], Yunlong Huo [a], Hui Lin [a]

[a] Third Institute of Oceanography, Ministry of Natural Resources, Xiamen 361005, China
[b] State Key Laboratory of Marine Environmental Science, Xiamen University, Xiamen 361102, China
[c] Guangxi Shankou Mangrove Nature Reserve, Beihai 536000, China

HIGHLIGHTS

- Sources and sinks of mercury in mangrove sediments were investigated.
- Tracing sources of mercury in seawater based on isotope mixing model.
- Hg isotope fractionation was used to understand Hg transformations in sediments.
- Hg isotope values indicate Hg exchange between seawater and sediment.
- Isotope homogeneity revealed relationships of Hg between seawater, air and plants.

GRAPHICAL ABSTRACT

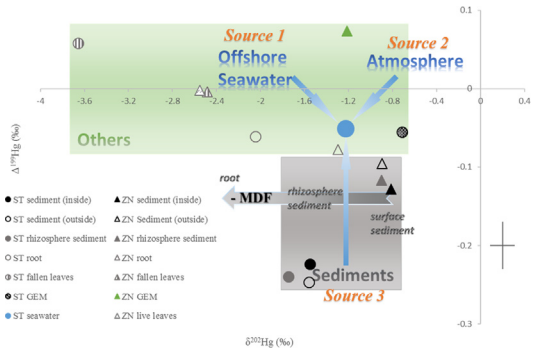

ARTICLE INFO

Article history:
Received 15 October 2019
Received in revised form 2 December 2019
Accepted 2 December 2019
Available online xxxx

Editor: Mae Sexauer Gustin

Keywords:
Tide
Seawater
Plants
MC-ICP-MS
Isotope mixing model

ABSTRACT

Mangrove forests are important wetland ecosystems that are a sink for mercury from tides, rivers and precipitation, and can also be sources of mercury production and export. Natural abundance mercury stable isotope ratios have been proven to be a useful tool to investigate mercury behavior in various ecosystems. In this study, mercury isotopic data were collected from seawater, sediments, air, and plant tissues in two mangrove forests in Guangxi and Fujian provinces, China, to study the transport and transformation of mercury in mangrove sediments. The mangroves were primarily subject to mercury inputs from external sources, such as anthropogenic activities, atmospheric deposition, and the surrounding seawater. An isotope mixing model based on mass independent fractionation (MIF) estimated that the mangrove wetland ecosystems accounted for <40% of the mercury in the surrounding seawater. The mercury in plant root tissues was derived mainly from sediments and enriched with light mercury isotopes. The exogenous mercury inputs from the fallen leaves were diluted by seawater, leading to a positive Δ^{199}Hg offset between the fallen leaves and sediments. Unlike river and lake ecosystems, mangrove ecosystems are affected by tidal action, and the δ^{202}Hg and Δ^{199}Hg values of sediments were more negative than that of the surrounding seawater. The isotopic signature differences between these environmental samples were partially due to isotope fractionation driven by various physical and chemical processes (e.g., sorption, photoreduction, deposition, and absorption). These results contribute to a better understanding of the biogeochemical cycling of mercury in mangrove wetland ecosystems.

© 2019 Elsevier B.V. All rights reserved.

* Corresponding author.
E-mail address: zhangyuanbiao@tio.org.cn (Y. Zhang).

https://doi.org/10.1016/j.scitotenv.2019.135928
0048-9697/© 2019 Elsevier B.V. All rights reserved.

1. Introduction

As a global pollutant, mercury can be released into the atmosphere through anthropogenic and natural sources and transported over long distances through atmospheric circulation (Driscoll et al., 2013; Strode et al., 2009). Although on a local scale, point sources of mercury may be important, mercury mainly enters the biosphere on a global scale in the form of atmospheric deposition and is converted into neurotoxic methylmercury, which is enriched in organisms through bioaccumulation (Mason et al., 1994; Mason and Sheu, 2002). As a global pollutant that is readily bioaccumulated, the transport and transformation of mercury has been a significant topic of international study.

Mangrove forests are important near-shore ecosystems that are considered to be sinks of many pollutants, including mercury (Sandilyan and Kathiresan, 2012; Vannucci, 2001). Hg(0) can be sequestered in the soil, and Hg(II) can enter the soil directly through dry and wet atmospheric deposition (Juillerat et al., 2012; Obrist et al., 2014). Mercury is absorbed into the leaves through a gas exchange process of the leaf stomata and enters the soil via fallen leaves (Grigal, 2002; Obrist et al., 2012). Mangrove wetland ecosystems are also a source of mercury (Galloway and Branfireun, 2004; Marchand et al., 2006). For example, mangrove plant debris releases mercury under anaerobic decomposition (Liu and Ding, 2007; St Louis et al., 1994); in wetlands, inorganic mercury is converted by microbes to methylmercury, which in turn is accumulated in the aquatic food chain (Hall et al., 2008).

The stable isotopes of mercury have proven to be an effective and reliable means of clarifying the transport and transformation of mercury in the environment. For example, the spatial distribution of mercury isotopic compositions in mineral soils across North American forests is modeled by isotopic mixing, assuming that atmospheric Hg(II), atmospheric Hg(0), and geogenic mercury are the major sources (Zheng et al., 2016). Data of the mercury isotopic signatures in soil and litterfall at Mt. Ailao in Southwestern China suggest that mercury in surface soils is mainly derived from litterfall mercury input and enhanced by precipitation (Wang et al., 2019). Variation in the mercury isotopic compositions of the dissolved and suspended fractions along the flow path of the East Fork Poplar Creek in Oak Ridge, Tennessee, was attributed to physical and in-stream processes with additional sources of dissolved mercury inputs at the baseflow that predominantly arose from the hyporheic zone (Demers et al., 2018).

Few researchers to date have studied mercury isotopes in mangrove ecosystems (Gao, 2015; Sun et al., 2017). Limited results showed that mercury was photoreduced before being enriched in mangrove plants (Sun et al., 2017). Mercury in mangrove leaves was mainly derived from the atmosphere, and mercury in the root tissue was mostly from the surface soil (Sun et al., 2017). Many remaining questions must be answered to understand the biogeochemical cycling of mercury in mangrove ecosystems, such as the mercury exchange between the seawater, plants, and sediment; as well as the primary factors that influence mercury species in mangrove ecosystems, e.g., photoreaction, microbial methylation, or other unknown processes; in addition, the differences between coastal systems with and without mangrove plants must be determined. In this study, samples of seawater, sediments, the atmosphere, plant root tissues, live leaves, and fallen leaves were collected from two mangrove areas in Guangxi and Fujian provinces, China, and analyzed for mercury isotopes. Using mercury stable isotopes technology, this study was performed to understand: (1) the effect of tide on the mercury exchange between seawater and sediment, and (2) the transport and transformation of mercury in mangrove sediments.

2. Materials and methods

2.1. Site descriptions and sampling

In October 2017, sampling was performed at Shatian Port (ST, 109.667°N, 21.555°E) in the Shankou Mangrove Reserve of Guangxi province, including 3 sampling sites inside the mangrove forest, 2 sites in the intertidal zone, and 14 sites in the estuary (Fig. 1). The samples consisted of (1) core and surface sediment, (2) sediments from the rhizosphere, (3) mangrove plant tissues, (4) seawater, and (5) atmospheric (gaseous) samples for elemental mercury (GEM) analysis. In May 2018, sampling was also performed in the mangrove forest at the Jiulong River Estuary, Zini Town, Fujian province (ZN, 117.906°N, 24.438°E), including 3 sampling sites inside the mangrove forest and 2 sites in the intertidal zone (Fig. 1). The samples consisted of core and surface sediments as well as rhizosphere sediments, mangrove plant samples, and GEM samples. The collected plant samples were of *Bruguiera gymnorrhiza*. As shown in Fig. 1, three sampling sites were located inside the mangrove forest and two sampling sites were established on the adjacent mud flat in the ST and ZN mangrove areas. Plant samples STB1 and STB2 were collected from STH1 and STH2, respectively. Plant samples ZNB1, ZNB2, ZNB3, and ZNB4 were collected from ZNG2, ZNH1, ZNH2, and ZNH3, respectively. Site ZNG2 was established on the adjacent mud flat, but it was close to the mangrove forest; the plant samples at ZNG2 were collected from the nearest mangrove plants. The ST mangrove area is located 60 km from the city of Beihai, and industrial activities (containing a coal-fired power plant) occur 10 km to the northwest. The ZN mangrove area is located 20 km to the west of the city of Xiamen, and 10 km to the east of the mangrove area is a large coal-fired power plant. The tidal conditions are regular semidiurnal and diurnal tide in the ZN and ST mangrove areas, respectively. The sampling was conducted during ebb conditions. The seawater sampling sites were distributed around the mangrove area and ~10 L surface seawater was collected at each site.

Core sediments were collected to depths of 20–60 cm with a PET sediment corer (10 cm diameter and 80 cm length). Core sediments were set as the central point at each site. Surface sediment was a homogenized composite consisting of four approximately 50-g samples that were taken within a 5-m radius at each site. The rhizosphere sediments were collected at the bottom of three plants around the core sediment and homogenized. According the previous data (Din et al., 2009), the sediments contained high proportion of sand. The plant samples were collected from at least three plants around the core sediment at each site. The sediment and plant samples were all collected with ceramic tools.

2.2. Sample pretreatment and analysis

Subsamples of the core sediments were collected at 5-cm intervals. Core sediments and plant samples were separately lyophilized, ground with a ball mill, passed through a 200-mesh sieve, and stored in double Ziplock bags in a desiccator. After digesting the samples with aqua regia ($HCl:HNO_3$, 3:1, *v/v*) at a high temperature, the solution was passed through a 0.22-μm filter (acetate cellulose membrane) and the filtrate was stored for analysis (Sonke et al., 2010). Seawater samples were fixed in the field with 0.5% (v/v) BrCl, brought back to the laboratory, pre-concentrated by a purge-and-trap with a potassium permanganate solution, and stored for analysis (Lin et al., 2015). The atmospheric GEM samples were collected using gold traps, and the mercury in the gold traps was transferred to a potassium permanganate solution by thermal desorption (Demers et al., 2015; Huang et al., 2016a). Additional details pertaining to the sample pretreatment methods are provided in the supporting information (SI) Text S1. The total mercury concentration of each sample was determined using an atomic fluorescence spectrometer (CVAFS, Brooks Rand Instruments, US). Standard samples were prepared and used following the NIST 1646a, BCR 482, and NIST 3133 standards for the sediment, plant, and seawater samples, respectively. Total mercury recovery of the samples (excluding GEM samples) ranged between 82% and 103%. All the vessels used in the experiment were made of borosilicate glass or PTFE, and

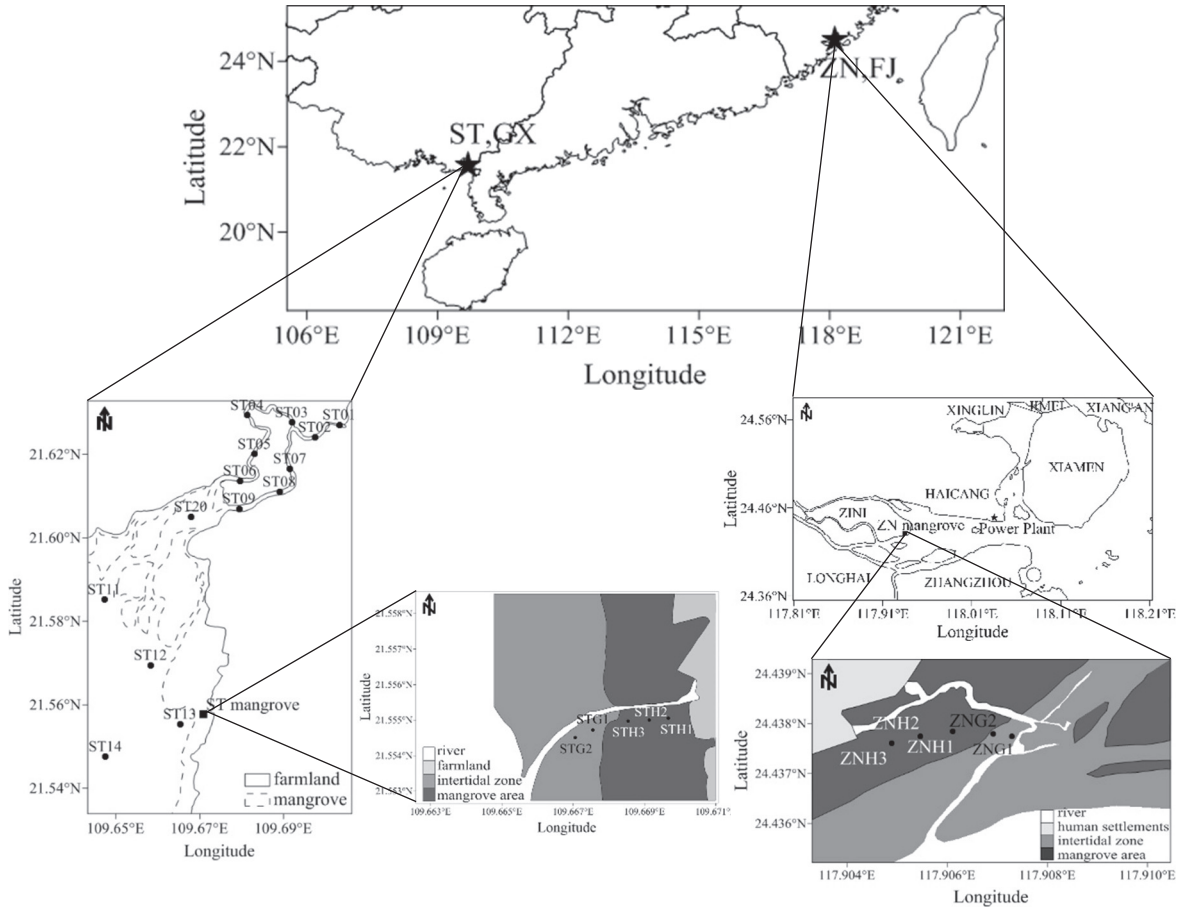

Fig. 1. Map of sampling sites.

cleaned thoroughly prior to use according to the US EPA (2002) Method 1631, Revision E. Mercury isotope ratios of the samples were determined using multi-collector inductively coupled plasma mass spectrometry (MC-ICP-MS, Nu Instruments, UK) (see SI Text S2) at the State Key Laboratory of Marine Environmental Science, Xiamen University.

3. Results and discussion

3.1. Total mercury concentration

As shown in Fig. 2, the average total mercury concentration in the core sediments from the mangrove forest at ST was 43 ± 27 ng/g

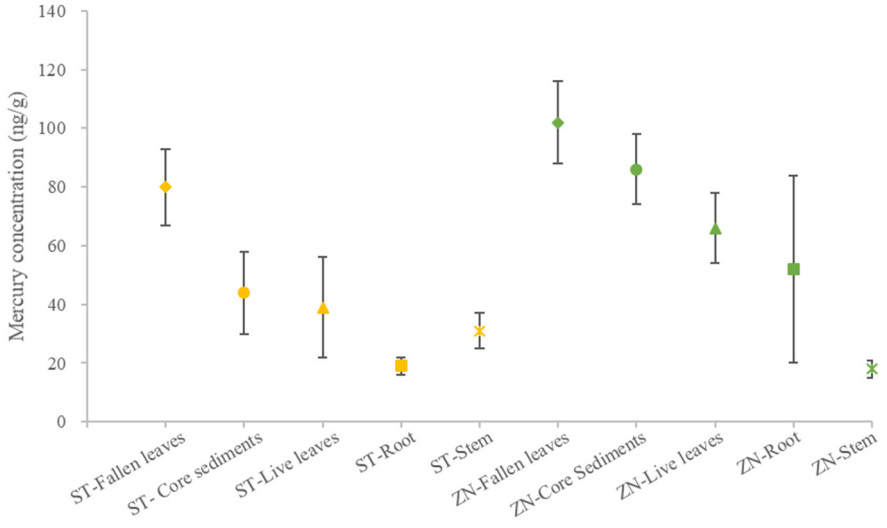

Fig. 2. Total mercury concentrations in all samples. The error bars on the Y axis are standard deviations of the mercury concentrations.

($n = 21$, SD), which was lower than that at ZN (86 ± 24 ng/g, $n = 59$, SD). Total mercury concentrations ranged from 11 to 97 ng/g and 24 to 120 ng/g at ST and ZN, respectively. The total mercury concentrations in the surface and rhizosphere sediments were higher at ST, with values of 75 ± 22 ng/g ($n = 3$, SD) and 74 ± 2 ng/g (n = 2, SD), respectively, whereas the mercury concentrations in the surface and rhizosphere sediments were lower at ZN, with values 53 ± 38 ng/g (n = 3, SD) and 73 ± 33 ng/g (n = 3, SD), respectively. The mercury concentration was lowest in the plant root and stem samples, with values of 17 ± 4 ng/g (n = 3, SD) and 31 ± 12 ng/g (n = 3, SD) at ST, respectively, and 52 ± 32 ng/g (n = 2, SD) and 20 ± 2 ng/g ($n = 4$, SD) at ZN, respectively. The mercury concentration range was large in the plant root samples, with a lower value (6 ng/g) in ZNB2 and a higher value (97 ng/g) in ZNB3. The highest mercury concentration was observed in the fallen leaves with values of 83 ± 26 ng/g (n = 3, SD) at ST and 102 ± 28 ng/g (n = 4, SD) at ZN. The total mercury concentration of the seawater at ST ranged from 0.84 to 11.21 ng/L.

Collected plant samples were mainly composed of fallen leaves, live leaves, roots, and stems. The fallen leaves had the highest mercury content, followed by sediment and live leaves, with the lowest levels of mercury in the roots and stems (Fig. 2). The results were consistent with previous findings that after withering and falling, mangrove leaves in a sedimentary environment is degraded and concentrated with mercury held to organic matter, thereby increasing the total mercury concentration of the fallen leaves above the observed concentrations in live leaves (Pokharel and Obrist, 2011).

3.2. Sources of mercury in seawater

The mercury isotopic composition of the seawater collected from the area surrounding the mangrove forest at site ST was measured (Fig. 3). The δ^{202}Hg and Δ^{199}Hg values of seawater were − 1.22 ± 0.30‰ (2SD, $n = 14$) and −0.05 ± 0.08‰ (2SD, n = 14), respectively. The MIF values of odd isotopes were slightly negative in the seawater samples, and the Δ^{199}Hg value at station ST13 was more negative (−0.16‰, Table S1). The MIF values of the even isotopes were slightly positive, but small in the seawater samples, suggesting that mercury in the seawater was likely to have been derived from atmospheric sources.

It is generally accepted that the main source of mercury in seawater is atmospheric deposition, and mercury exchange between the seawater and underlying sediments provides another source of mercury in the seawater (Delongchamp et al., 2010). Due to the effect of tides, mercury exchange also takes place between the surface sediments of mangrove forests and the surrounding seawater. Studies have shown that during this process, seawater extracts mercury from wetland sediments and pore waters during high tides and transports mercury back to coastal waters at low tides (Bergamaschi et al., 2012; Shanley et al., 2008). Mercury in estuarine areas and adjacent mangrove ecosystems may even be transported to the continental shelf (Araujo et al., 2017). Therefore, we considered atmospheric deposition and surface sediment as the two main sources of mercury in the seawater.

Using the published mercury isotope data of atmospheric mercury species (Gratz et al., 2010; Huang et al., 2018; Sun et al., 2016), it is possible to deduce the approximate range in the mercury isotopic composition of precipitation within the ST mangrove area (more details in SI Text S3). The isotopic data for precipitation can be combined with the isotopic data from the surface sediments inside the ST mangrove area (referred to as mangrove sediments, marked by filled triangle in Fig. 3) to develop an isotope mixing model that estimates the contribution of mercury to seawater from mangrove sediments and precipitation. In addition, because the mercury in seawater and precipitation may undergo photochemical reactions leading to MDF, only Δ^{199}Hg was used in the model, as follows:

$$\Delta^{199}_{seawater} = f_{sediment} \times \Delta^{199}_{sediment} + (1 - f_{sediment}) \times \Delta^{199}_{precipitation},$$

where $\Delta^{199}_{seawater}$, $\Delta^{199}_{sediment}$, and $\Delta^{199}_{precipitation}$ represent the Δ^{199}Hg values of the surrounding seawater, mangrove sediment, and precipitation, respectively; and $f_{sediment}$ represents the contribution of the mercury input from mangrove sediment to the surrounding seawater. The results showed that, except for the seawater sample at station ST13, most (>60%) of the mercury in seawater was from atmospheric precipitation, as listed in Table S1. The seawater sample at station ST13 was

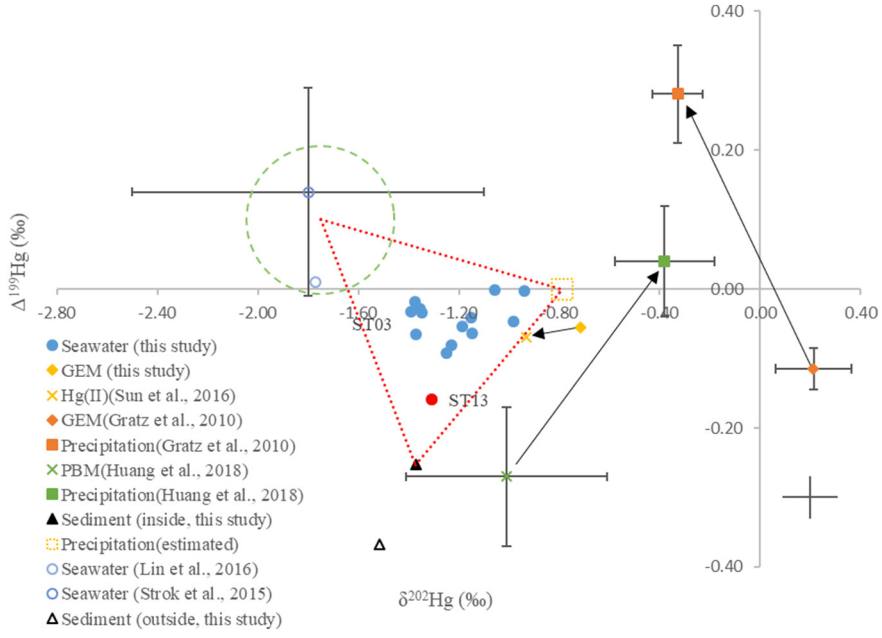

Fig. 3. Mercury isotopic composition of seawater near the ST mangrove forest and its relationship with that of the GEM and surface soils. The dashed circle represents the estimated isotopic composition of the seawater. The error bars on the right bottom are analytical uncertainties of δ^{202}Hg and Δ^{199}Hg defined in the Materials and Methods section. The error bars on the data points are analytical uncertainties reported previously (Hg(II) from Sun et al. (2016), GEM and precipitation from Gratz et al. (2010), PBM and precipitation from Huang et al. (2018), and seawater from Lin et al. (2016) and Štrok et al. (2015)).

more affected by the mangrove sediments than the other seawater samples were, because sampling site ST13 was located closest to the mangrove forest. The contribution of the mercury input from mangrove sediments to the surrounding seawater decreased from 0.59% to 0.30% as the distance from the sampling site to the mangrove area increased. Moreover, the contribution was <0.30% at sites located in the continental river.

A previous study showed that due to the low permeability of clay sediments, most of the precipitation does not penetrate into the ground, but flows directly into the seawater over the land surface (McGowan and Martin, 2007). Thus, the influence of precipitation on the seawater is not only from the atmosphere, but also from the surrounding surficial soil. Because the influence of precipitation on the sediments would be minimized by plant cover, the surface sediments on an adjacent mud flat outside the ST mangrove area (marked with open triangles in Fig. 3) were used instead of the mangrove sediments as the end member to calculate the contribution of mercury from these sediments to the surrounding seawater using the equation above. The amounts of mercury were lower than those of previous analyses, indicating that more mercury in the seawater was derived from atmospheric precipitation (Table S1). This indicated that the mangrove plants affected the transfer of mercury from the atmosphere to the sediments, and thus decreased the contribution of mercury from the atmosphere to the surrounding seawater.

For the convenience of calculation, it was assumed that the mercury in the seawater was originated from atmospheric deposition and surrounding sediments, but the input of mercury from offshore seawater to coastal waters cannot be ignored. As shown in Fig. 3, the mercury isotopic composition of seawater surrounding the ST mangrove area fell within the triangular dashed box formed by the data of these three sources. The background mercury isotope signatures of the seawater that was not subject to point-source mercury pollution from a coal-fired power plant were reported to be $\delta^{202}Hg = -1.77‰$ and $\Delta^{199}Hg = 0.01‰$ (Lin et al., 2016). Coastal waters in the Arctic are less polluted by anthropogenic mercury and show large negative MDF and positive MIF values ($\delta^{202}Hg = -1.80 \pm 0.70‰$, $\Delta^{199}Hg = 0.14 \pm 0.15‰$, $n = 21$) (Štrok et al., 2015). In addition, the mercury isotopic composition of sediments that were far offshore and far from mercury pollution also showed positive MIF values (Foucher et al., 2013; Mil-Homens et al., 2013; Yin et al., 2015). Unfortunately, it would be impossible to estimate the input of mercury from offshore seawater to coastal waters without first knowing the mercury isotopic composition of the offshore seawater in this area. However, it is likely that the mercury contribution from the mangrove sediments to the surrounding seawater would be lower based on the three-end member isotope mixing model:

$$\Delta^{199}_{seawater} = f_{sediment} \times \Delta^{199}_{sediment} + \left(1 - f_{sediment} - f_{offshore}\right) \times \Delta^{199}_{precipitation} + f_{offshore} \times \Delta^{199}_{offshore},$$

where $\Delta^{199}_{offshore}$ represents the $\Delta^{199}Hg$ of the offshore seawater, and $f_{offshore}$ represents the contribution of mercury from the offshore seawater to the surrounding seawater. Therefore, it can be inferred that in this area, <40% of the mercury in the surrounding seawater was derived from the mangrove sediments. Furthermore, the tides were falling when the samples were collected, and mercury input to the seawater from the sediments would be smaller when the tides were rising.

Similar patterns were also observed in the ZN mangrove area, as shown in Table S2. According to the above model, without considering the influence of offshore seawater, the input of mercury from the ZN mangrove sediments to the surrounding seawater was estimated to be 19%. The results in the ZN and ST mangroves were consistent. Further work must focus on the relationship between the contribution of mercury from mangrove ecosystems to the surrounding seawater and geographic factors, such as topography, tidal elevation, and sediment types.

3.3. Transport and transformation of mercury in sediments

As shown in Fig. 4, the isotopic composition of the sediments in the ST and ZN mangrove areas were quite different and exhibited large ranges, with values of $-1.08 \pm 0.82‰$ ($n = 82$, 2SD) for $\delta^{202}Hg$ and $-0.15 \pm 0.15‰$ (n = 82, 2SD) for $\Delta^{199}Hg$. Most of the negative isotopic signatures were observed in sediments of the ST mangrove area. The spatial variation of mercury isotopic compositions could be caused by variations in mercury sources or differences in the transformations.

Mercury isotopic compositions of the soils in urban and industrial areas vary based on the degree of anthropogenic mercury pollution, but the overall difference is small. Soils in remote areas that are minimally affected by human activities and remain relatively pristine, such as mountain soils (Biswas et al., 2008; Zhang et al., 2013), forest soils (Demers et al., 2013; Jiskra et al., 2015; Woerndle et al., 2018; Zheng et al., 2016), and the Qinghai–Tibet Plateau soils (Wang et al., 2017), have unique mercury isotopic compositions ($\delta^{202}Hg = -1.82 \pm 0.39‰$, $\Delta^{199}Hg = -0.29 \pm 0.12‰$, 1SD, $n = 156$) (Yin et al., 2018). Mercury isotopes in urban soils exhibit slightly negative MDF values ($\delta^{202}Hg = -0.64 \pm 0.27‰$, 1SD, $n = 18$) and near-zero MIF values ($\Delta^{199}Hg = -0.01 \pm 0.07‰$, 1SD, n = 18) (Estrade et al., 2011; Huang et al., 2016b), indicating that while urban areas are more directly affected by anthropogenic activities, the mercury pollution is not severe. The areas most affected by anthropogenic mercury pollution include areas of mercury (gold) amalgamation mining areas, smelters, wastewater treatment plants, and waste incinerators, where the mercury isotopic compositions of the soils show slightly positively shifted MDF values ($\delta^{202}Hg = -0.55 \pm 0.30‰$, 1SD, $n = 32$) and MIF values ($\Delta^{199}Hg = 0.03 \pm 0.05‰$, 1SD, n = 32) compared with urban soils (Donovan et al., 2016; Estrade et al., 2011; Kwon et al., 2014).

As shown in Fig. 4, the mercury isotopic compositions of the sediments possessed regional characteristics. The $\delta^{202}Hg$ and $\Delta^{199}Hg$ of the ST mangrove sediments ranged from $-1.90‰$ to $-0.99‰$ and from $-0.39‰$ to 0.01‰, respectively, while the ZN mangrove sediments ranged from $-1.40‰$ to $-0.27‰$ and from $-0.22‰$ to $-0.04‰$, respectively. Mercury isotopic compositions of the ZN mangrove sediments were more closely related to industrial and urban soils, while those of the ST mangrove sediments were closer to those of forest soils, indicating that the ZN mangrove sediments were more affected by anthropogenic mercury pollution than the ST mangrove sediments. The main commonality with forest soils is that they have vegetation cover. Therefore, the sources of mercury include decayed plant tissues, atmospheric

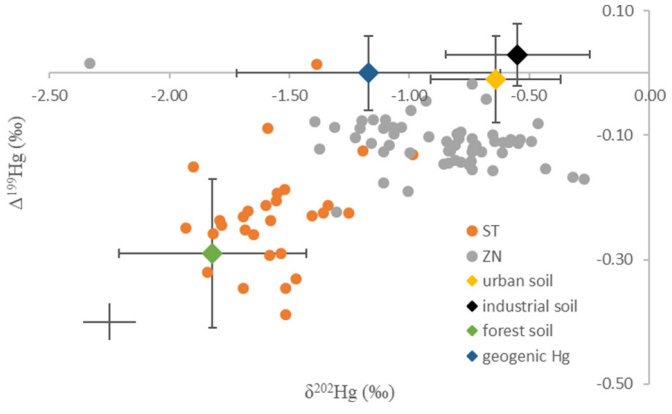

Fig. 4. Mercury isotopic composition of sediments. The error bars on the left bottom are analytical uncertainties of $\delta^{202}Hg$ and $\Delta^{199}Hg$ defined in the Materials and Methods section. The error bars on the data points represent 2SD, calculated from data reported previously (urban soil (Estrade et al., 2011; Huang et al., 2016b); industrial soil (Donovan et al., 2016; Estrade et al., 2011; Kwon et al., 2014); forest soil (Biswas et al., 2008; Demers et al., 2013; Jiskra et al., 2015; Wang et al., 2017; Woerndle et al., 2018; Yin et al., 2018; Zhang et al., 2013; Zheng et al., 2016); data pertaining to mercury of geological origin (Yin et al., 2012, 2016)).

deposition, and mercury of geological origin. However, current research suggests that mercury of geological origin is not the main source of mercury in forest sediments (Fiorentino et al., 2011; Grimaldi et al., 2008; Peña-Rodríguez et al., 2014). Studies using geochemical ratios to trace the sources of soil mercury have shown that mercury in surface soils are mainly affected by external factors (such as the atmosphere) rather than geological sources (Fiorentino et al., 2011; Grimaldi et al., 2008; Peña-Rodríguez et al., 2014).

In addition to the above sources, seawater is the most significant source of mercury in mangrove ecosystems, differing from forest ecosystems. Under the influence of tides, mercury isotopic compositions of mangrove sediments are affected by seawater. Studies have shown that sediments covered by estuarine water (Gao, 2015; Lin, 2015), lake water (Chen et al., 2016), and river water (Demers et al., 2018; Donovan et al., 2014) have significantly different mercury isotopic compositions than the water itself (Fig. 5). This difference is mainly related to the sources of mercury in the water and sediments. The surrounding seawater in the ST mangrove area had higher Δ^{199}Hg values relative to the values in the sediments. The observed difference in the isotopic values may be related to several sources. First, seawater receives mercury inputs from atmospheric deposition that possesses positive Δ^{199}Hg values. Second, in water (including precipitation), dissolved mercury displays more positive Δ^{199}Hg values than particulate mercury (Demers et al., 2015, 2018; Lin et al., 2015), the latter of which is more likely to be preserved in sediments. Because a mangrove forest mainly grows above the mean sea level and below the high-tide line of an estuary, the mangrove sediments are gradually submerged by seawater only during high tides. Therefore, when the tides rise and the area is inundated with seawater, particulate mercury with negative Δ^{199}Hg values may be deposited over the mangrove sediments. In addition, when the tides are falling, the dissolved mercury in the pore waters of the sediments is removed, mixed with the seawater, and transported from the area that increases the MIF values of the seawater relative to those of the mangrove sediments. Previous research has shown that mangrove forests are one of the sources of reactive mercury (i.e., Hg(II), dissolved gaseous mercury, and mercury weakly bound to complexes) in the surrounding seawater (Lacerda et al., 2001).

Another explanation for the different Δ^{199}Hg values between seawater and sediment is that mercury in the seawater and sediments has undergone varying degrees of photoreduction. We supposed that more mercury was photoreduced in the seawater than in the sediment, as the sediments were covered by mangrove plants. To date, the photoreduction reactions that have been demonstrated to cause large positive MIF values deplete light mass isotopes in the residual Hg(II) phase (Bergquist and Blum, 2007; Zheng and Hintelmann, 2009, 2010a). Therefore, it was inferred that the mercury in the seawater exhibited more positive Δ^{199}Hg and δ^{202}Hg values than mercury in sediments, which was consistent with our results. However, photoreduction is not likely to be the primary process occurring in sediments, since the surficial sediment uncovered near the mangrove plants did not show significantly different isotope signatures from that of the sediment inside the mangrove area.

The ST mangrove sediments had more negative δ^{202}Hg values than the surrounding seawater. This pattern differed from the results of freshwater and nearshore water (Fig. 5). Mangrove sediments are different from aquatic sediments in that they are not always covered by water. We hypothesized that when the tides are low, mercury in the mangrove sediments are photoreduced, and a fraction of the Hg(0) is directly released into the atmosphere. When seawater inundates the mangrove sediments, Hg(II) in the sediments with relatively positive δ^{202}Hg values undergoes an exchange with the seawater, shifting the δ^{202}Hg in seawater to more positive values relative to that before the rise in the tide. Under the influence of tides, the seawater around the mangroves will gradually have δ^{202}Hg values that are positively shifted relative to those of the mangrove sediments.

A similar pattern was observed in the bank porewater of the South River, Virginia by Washburn et al. (2017). The authors attributed the positive δ^{202}Hg shift between suspended and dissolved bank porewater mercury to two fractionation processes. The first process was photoreduction, as we suggested. The second process was the sorption of mercury in the dissolved phase to particulates, including Fe oxides and thiol functional groups (Jiskra et al., 2012; Wiederhold et al., 2010). This interpretation was neither supported here nor the main process occurring in the sediment, because the MIF of mercury observed during mercury-thiol complexation was induced by nuclear volume effect, which was not observed in this study.

3.4. Effects of plants on mercury in sediments

The mercury isotopic composition of the mangrove core sediments did not change significantly with depths below 10 cm (Fig. S1). This observation is consistent with an earlier study (Zheng et al., 2016), indicating that depth has a minimal effect on the mercury isotopic composition of mangrove sediments. Moreover, the data suggest that mangrove sediments retain the mercury isotope information acquired prior to burial over long temporal scales. However, the rhizosphere sediments had more negative δ^{202}Hg values (ST, -1.74 ± 0.11‰; ZN, -0.90 ± 0.42‰) than the associated surface sediments (ST, -1.55 ± 0.13‰; ZN, -0.70 ± 0.08‰) (Fig. 6). In general, plants absorb heavy metals from the surrounding soils through the roots (Yoon et al., 2006). As

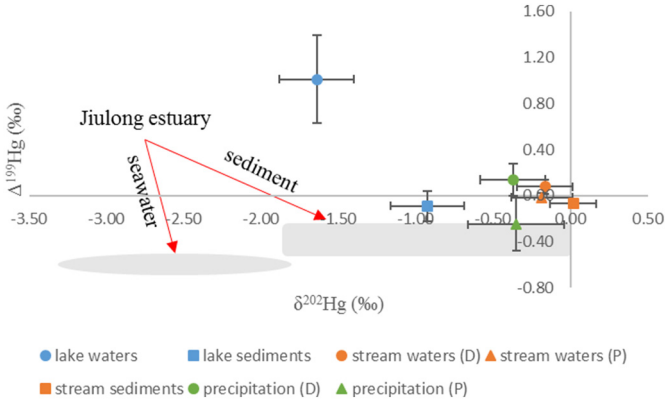

Fig. 5. Mercury isotopic composition of water and sediments (D and P represent dissolved and particulate mercury, respectively). The error bars on the data points represent 2SD, calculated from data reported previously (lake water and lake sediments (Chen et al., 2016), river water (Demers et al., 2018), river sediments (Donovan et al., 2014), precipitation (Huang et al., 2018), seawater from the Jiulong River Estuary (the gray ellipse) (Lin, 2015), and Jiulong River Estuary sediments (the gray rectangle) (Gao, 2015)).

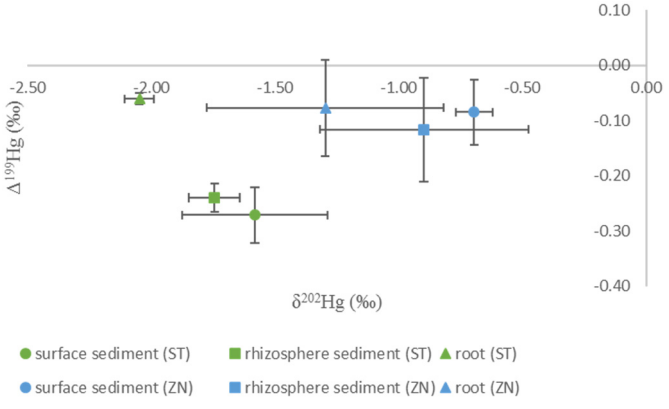

Fig. 6. Mercury isotopic composition of surface sediments, rhizosphere sediments, and plant roots. The error bars on the data points represent 2SD, calculated using the data from this study.

shown in Fig. 6, the largest negative δ^{202}Hg values were observed in plant root tissues, which is consistent with the changes in signs to negative δ^{202}Hg values between the sediments and roots observed in mangrove and rice plants (Sun et al., 2017; Yin et al., 2013). This indicates that in the process of mercury uptake by plant roots, light mercury isotopes are preferentially absorbed by the plants, which enriches the mangrove sediments in the heavy mercury isotopes to some extent.

As an important means for mangrove plants to return mercury to the sediments, fallen leaves exhibited negative δ^{202}Hg values (−3.66‰ to −2.19‰) and distinctly positive Δ^{199}Hg values (−0.08‰ to 0.10‰) relative to those of sediments (Fig. 7). In forest ecosystems, the main source of mercury in fallen leaves is GEM, which has large negative Δ^{199}Hg values (Demers et al., 2013; Yu et al., 2016; Zheng et al., 2016). However, in mangrove ecosystems, when leaves fall to the soil, the effects of atmospheric inputs on the fallen leaves are diluted by tidal action, resulting in insignificant differences in the Δ^{199}Hg values between GEM, the seawater, and the fallen leaves. The fallen and live leaves in the ZN mangrove area had similar mercury isotopic compositions (Fig. 7), because the fallen leaves were so fresh that emission, retention, and sorption of mercury were insufficient to alter the isotopic signatures. Otherwise, mercury enriched in older and more decomposed leaves would be accompanied by a positive shift of δ^{202}Hg and small negative Δ^{199}Hg values (Jiskra et al., 2015; Zheng et al., 2016). In contrast, an increase in Δ^{199}Hg from 1 to 10 cm was observed in the core sediments (Fig. S1), further indicating the dilution effect of the tidal action on the exchange of mercury between fallen leaves and sediments. However, this implies that dark redox reactions likely induce the lower Δ^{199}Hg in surficial sediments, because experimental studies have shown that these processes either produce no MIF or negative MIF in the Hg(II) phase in surficial sediment (Kritee et al., 2008, 2013; Zheng and Hintelmann, 2010b; Zheng et al., 2019). The large difference in the Δ^{199}Hg values between the fallen leaves and sediments also indicates that mercury exchange between the leaves and the sediments was insignificant, and that the sources of mercury were different. As discussed earlier, the mercury in mangrove sediments is mainly derived from particulate mercury (Hg(II)) with more negative Δ^{199}Hg values, and the mercury in fallen leaves is mainly derived from GEM (Hg(0)). Thus, the positive Δ^{199}Hg in fallen leaves is affected by the deposition of Hg(0) and subsequent mixing with seawater.

Overall, our observations of the mercury isotopic compositions associated with sediments in the mangrove demonstrated that the mercury in the sediments was derived from several sources (e.g., atmospheric deposition, mercury pollution sources, and seawater) and underwent various physical and chemical processes (e.g., sorption, photoreduction, dark reduction, and oxidation). These source- and process-driven mechanisms partially explain why sediments within mangrove and forest ecosystems have negative δ^{202}Hg values relative to those generally found in river and lake sediments. For example, δ^{202}Hg in river sediments in Tennessee, USA, ranged from −1.6‰ to −0.1‰ (Bartov et al., 2013); δ^{202}Hg in lake sediments of central Florida ranged from −1.19‰ to −0.65‰ (Sherman and Blum, 2013); δ^{202}Hg in estuary sediments in New Jersey, USA ranged from −0.48‰ to −0.21‰ (Janssen et al., 2015); δ^{202}Hg in sediments of the Great Lakes of North America ranged from −1.42‰ to −0.14‰ (Lepak et al., 2015).

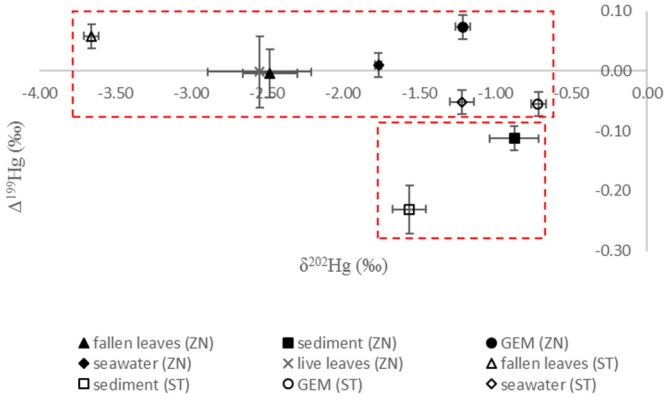

Fig. 7. Mercury isotopic composition of fallen leaves and their surrounding sediments, the atmosphere, and seawater. The error bars represent either 2SD calculated from data in this study or analytical uncertainties of δ^{202}Hg and Δ^{199}Hg defined in the Materials and Methods section.

4. Environmental implications

The mercury isotopic compositions of seawater, sediments, and plant tissues in the studied mangrove areas varied widely as a function of the sources of mercury in each component. The spatial distribution in the mercury content and isotopic composition of the mangrove sediments with depth did not exhibit large changes, indicating that the mercury sources of the mangrove wetland ecosystem and isotope fractionation processes were relatively stable over a long time. In general, the mercury isotopic composition of mangrove sediments is closely related to multiple sources of mercury, such as GEM, atmospheric precipitation, surrounding seawater, anthropogenic activities, plant debris, and geological materials. It is widely accepted that GEM is the main source of mercury in forest soils, but in mangrove ecosystems, the surrounding seawater has a larger impact on the mercury content and isotopic composition of mangrove sediments through tidal action. Seawater transports particulate mercury to mangrove sediments during high tides; however, when the tides are falling, seawater removes dissolved mercury and volatile Hg(0) from mangrove sediments. Based on an isotope mixing model that used surface sediments, atmospheric precipitation and offshore seawater as three end members, it was estimated that the percentage contribution of mercury from the mangrove sediments to the surrounding seawater was below 40% and decreased with distance. These findings clarify the transport and transformation of mercury in sediment, lay a foundation for establishing a mercury isotope database for mangrove wetland ecosystems, and facilitate an understanding of the biogeochemical cycling of mercury.

Notes

The authors declare no competing financial interest.

Declaration of competing interest

The authors declare no conflict of interest.

Acknowledgements

This research was financed by the Scientific Research Foundation of the Third Institute of Oceanography, Ministry of Natural Resources, China (No. 2016045; No. 2016014). The authors thank the State Key Laboratory of Marine Environmental Science, Xiamen University, for support during the mercury isotope analyses, and LetPub (www.letpub.com) for providing linguistic assistance during the preparation of this manuscript.

Appendix A. Supplementary data

Sample pretreatment method (Text S1). Mercury isotope analysis (Text S2). Detailed deduction process of the estimated mercury isotopic composition of precipitation within the ST mangrove area (Text S3). Results from isotope mixing model (Table S1). Δ^{199}Hg values of ST and ZN mangrove sediments and their surrounding seawater and atmosphere (Table S2). Mercury isotope compositions for all the samples in this study (Table S3). Plot of mercury concentration, δ^{202}Hg, and Δ^{199}Hg versus depth in the core sediments (Fig. S1).The following are the

supplementary data related to this article. Supplementary data to this article can be found online at https://doi.org/10.1016/j.scitotenv.2019.135928

References

Araujo, B.F., Hintelmann, H., Dimock, B., Almeida, M.G., Rezende, C.E., 2017. Concentrations and isotope ratios of mercury in sediments from shelf and continental slope at Campos Basin near Rio de Janeiro, Brazil. Chemosphere 178, 42–50.

Bartov, G., Deonarine, A., Johnson, T.M., Ruhl, L., Vengosh, A., Hsu-Kim, H., 2013. Environmental impacts of the Tennessee valley authority Kingston coal ash spill. 1. Source apportionment using mercury stable isotopes. Environ. Sci. Technol. 47, 2092–2099.

Bergamaschi, B.A., Krabbenhoft, D.P., Aiken, G.R., Patino, E., Rumbold, D.G., Orem, W.H., 2012. Tidally driven export of dissolved organic carbon, total mercury, and methylmercury from a mangrove-dominated estuary. Environ. Sci. Technol. 46, 1371–1378.

Bergquist, B.A., Blum, J.D., 2007. Mass-dependent and -independent fractionation of Hg isotopes by photoreduction in aquatic systems. Science 318, 417–420.

Biswas, A., Blum, J.D., Bergquist, B.A., Keeler, G.J., Xie, Z., 2008. Natural mercury isotope variation in coal deposits and organic soils. Environ. Sci. Technol. 42 (22), 8308–8309.

Chen, J.B., Hintelmann, H., Zheng, W., Feng, X., Cai, H., Wang, Z., Yuan, S., Wang, Z., 2016. Isotopic evidence for distinct sources of mercury in lake waters and sediments. Chem. Geol. 426, 33–44.

Delongchamp, T.M., Ridal, J.J., Lean, D.R.S., Poissant, L., Blais, J.M., 2010. Mercury transport between sediments and the overlying water of the St. Lawrence River area of concern near Cornwall, Ontario. Environ. Pollut. 158, 1487–1493.

Demers, J.D., Blum, J.D., Zak, D.R., 2013. Mercury isotopes in a forested ecosystem: implications for air-surface exchange dynamics and the global mercury cycle. Glob. Biogeochem. Cycles 27, 222–238.

Demers, J.D., Sherman, L.S., Blum, J.D., Marsik, F.J., Dvonch, J.T., 2015. Coupling atmospheric mercury isotope ratios and meteorology to identify sources of mercury impacting a coastal urban-industrial region near Pensacola, Florida, USA. Glob. Biogeochem. Cycles 29, 1689–1705.

Demers, J.D., Blum, J.D., Brooks, S.C., Donovan, P.M., Riscassi, A.L., Miller, C.L., Zheng, W., Gu, B., 2018. Hg isotopes reveal in-stream processing and legacy inputs in East Fork Poplar Creek, Oak Ridge, Tennessee, USA. Environ. Sci. Process Impacts 20 (4), 686–707.

Din, Z.H., Liu, J.L., Li, L.Q., Lin, H.N., Wu, H., Hu, Z.Z., 2009. Distribution and speciation of mercury in surficial sediments from main mangrove wetlands in China. Mar. Pollut. Bull. 58, 1319–1325.

Donovan, P.M., Blum, J.D., Demers, J.D., Gu, B., Brooks, S.C., Peryam, J., 2014. Identification of multiple mercury sources to stream sediments near Oak Ridge, TN, USA. Environ. Sci. Technol. 48, 3666–3674.

Donovan, P.M., Blum, J.D., Singer, M.B., Marvin-DiPasquale, M., Tsui, M.T.K., 2016. Isotopic composition of inorganic mercury and methylmercury downstream of a historical gold mining region. Environ. Sci. Technol. 50, 1691–1702.

Driscoll, C.T., Mason, R.P., Chan, H.M., Jacob, D.J., Pirrone, N., 2013. Mercury as a global pollutant: sources, pathways and effects. Environ. Sci. Technol. 47 (10), 4967–4983.

Estrade, N., Carignan, J., Donard, O.F.X., 2011. Tracing and quantifying anthropogenic mercury sources in soils of northern France using isotopic signatures. Environ. Sci. Technol. 45, 1235–1242.

Fiorentino, J.C., Enzweiler, J., Angelica, R.S., 2011. Geochemistry of mercury along a soil profile compared to other elements and to the parental rock: evidence of external input. Water Air Soil Pollut. 221 (1–4), 63–75.

Foucher, D., Hintelmann, H., Al, T.A., MacQuarrie, K.T., 2013. Mercury isotope fractionation in waters and sediments of the Murray Brook mine watershed (New Brunswick, Canada): tracing mercury contamination and transformation. Chem. Geol. 336, 87–95.

Galloway, M.E., Branfireun, B.A., 2004. Mercury dynamics of a temperate forested wetland. Sci. Total Environ. 325, 239–254.

Gao, Y., 2015. Study on Temporal and Spatial Variation of Mercury in Sediments of Jiulongjiang Estuary. Master dissertation. Xiamen University (in Chinese with English Abstract).

Gratz, L.E., Keeler, G.J., Blum, J.D., Sherman, L.S., 2010. Isotopic composition and fractionation of mercury in Great Lakes precipitation and ambient air. Environ. Sci. Technol. 44 (20), 7764–7770.

Grigal, D.F., 2002. Inputs and outputs of mercury from terrestrial watersheds: a review. Environ. Rev. 10 (1), 1–39.

Grimaldi, C., Grimaldi, M., Guedron, S., 2008. Mercury distribution in tropical soil profiles related to origin of mercury and soil processes. Sci. Total Environ. 401 (1–3), 121–129.

Hall, B.D., Aiken, G.R., Krabbenhoft, D.P., Marvin-DiPasquale, M., Swarzenski, C.M., 2008. Wetlands as principal zones of methylmercury production in southern Louisiana and the Gulf of Mexico region. Environ. Pollut. 154, 124–134.

Huang, S., Lin, K., Yuan, D., Gao, Y., Sun, L., 2016a. Mercury isotope fractionation during transfer from post-desulfurized seawater to air. Mar. Pollut. Bull. 113, 81–86.

Huang, Q., Chen, J., Huang, W., Fu, P., Guinot, B., Feng, X., Shang, L., Wang, Z., Wang, Z., Yuan, S., Cai, H., Wei, L., Yu, B., 2016b. Isotopic composition for source identification of mercury in atmospheric fine particles. Atmos. Chem. Phys. 16, 11773–11786.

Huang, S., Sun, L., Zhou, T., Yuan, D., Du, B., Sun, X., 2018. Natural stable isotopic compositions of mercury in aerosols and wet precipitations around a coal-fired power plant in Xiamen, southeast China. Atmos. Environ. 173, 72–80.

Janssen, S.E., Johnson, M.W., Blum, J.D., Barkay, T., Reinfelder, J.R., 2015. Separation of monomethylmercury from estuarine sediments for mercury isotope analysis. Chem. Geol. 411, 19–25.

Jiskra, M., Wiederhold, J.G., Bourdon, B., Kretzschmar, R., 2012. Solution speciation controls mercury isotope fractionation of hg(II) sorption to goethite. Environ. Sci. Technol. 46, 6654–6662.

Jiskra, M., Wiederhold, J.G., Skyllberg, U., Kronberg, R.M., Hajdas, I., Kretzschmar, R., 2015. Mercury deposition and re-emission pathways in boreal forest soils investigated with Hg isotope signatures. Environ. Sci. Technol. 49, 7188–7196.

Juillerat, J.I., Ross, D.S., Bank, M.S., 2012. Mercury in litterfall and upper soil horizons in forested ecosystems in Vermont, USA. Environ. Toxicol. Chem. 31 (8), 1720–1729.

Kritee, K., Blum, J.D., Barkay, T., 2008. Mercury stable isotope fractionation during reduction of Hg(II) by different microbial pathways. Environ. Sci. Technol. 42, 9171–9177.

Kritee, K., Blum, J.D., Reinfelder, J.R., Barkay, T., 2013. Microbial stable isotope fractionation of mercury: a synthesis of present understanding and future directions. Chem. Geol. 336, 13–25.

Kwon, S.Y., Blum, J.D., Chen, C.Y., Meattey, D.E., Mason, R.P., 2014. Mercury isotope study of sources and exposure pathways of methylmercury in estuarine food webs in the northeastern U.S. Environ. Sci. Technol. 48, 10089–10097.

Lacerda, L.D., Silva, L.F.F., Marins, R.V., Mounier, S., Paraquetti, H.H.M., Benaim, J., 2001. Dissolved mercury concentrations and reactivity in mangrove waters from the Itacurussa Experimental Forest, Sepetiba Bay, SE Brazil. Wetl. Ecol. Manag. 9, 323–331.

Lepak, R.F., Yin, R., Krabbenhoft, D.P., Ogorek, J.M., DeWild, J.F., Holsen, T.M., Hurley, J.P., 2015. Use of stable isotope signatures to determine mercury sources in the Great Lakes. Environ. Sci. Technol. Lett. 2, 335–341.

Lin, H., 2015. Study of the Impact of Mercury in Post-Desulfurization Seawater Discharged from a Coal-Fired Power Plant onto the Discharging Sea Area Using Stable Isotopic Tracing Technique. PhD dissertation. Xiamen University (in Chinese with English Abstract).

Lin, H., Yuan, D., Lu, B., Huang, S., Sun, L., Zhang, F., Gao, Y., 2015. Isotopic composition analysis of dissolved mercury in seawater with purge and trap pre-concentration and a modified Hg introduction device for MC-ICP-MS. J. Anal. At. Spectrom. 30, 353–359.

Lin, H., Peng, J., Yuan, D., Lu, B., Lin, K., Huang, S., 2016. Mercury isotope signatures of seawater discharged from a coal-fired power plant equipped with a seawater flue gas desulfurization system. Environ. Pollut. 214, 822–830.

Liu, J.L., Ding, Z.H., 2007. Progress in research on mercury methylation in environment. Earth Environ. 35, 215–222 (in Chinese with English abstract).

Marchand, C., Lallier-Vergès, E., Baltzer, F., Albéric, P., Cossa, D., Baillif, P., 2006. Heavy metals distribution in mangrove sediments along the mobile coastline of French Guiana. Mar. Chem. 98, 1–17.

Mason, R.P., Sheu, G.R., 2002. Role of the ocean in the global mercury cycle. Glob. Biogeochem. Cycles 16 (4), 1093.

Mason, R.P., Fitzgerald, W.F., Morel, F.M.M., 1994. The biogeochemical cycling of elemental mercury: anthropogenic influences. Geochim. Cosmochim. Acta 58 (15), 3191–3198.

McGowan, K.T., Martin, J.B., 2007. Chemical composition of mangrove-generated brines in Bishop Harbor, Florida: interactions with submarine groundwater discharge. Mar. Chem. 104 (1), 58–68.

Mil-Homens, M., Blum, J., Canario, J., Caetano, M., Costa, A.M., Lebreiro, S.M., Trancoso, M., Richter, T., Stigter, H., Johnson, M., Branco, V., Cesario, R., Mouro, F., Mateus, M., Boer, W., Melo, Z., 2013. Tracing anthropogenic Hg and Pb input using stable Hg and Pb isotope ratios in sediments of the central Portuguese Margin. Chem. Geol. 336, 62–71.

Obrist, D., Johnson, D.W., Edmonds, R.L., 2012. Effects of vegetation type on mercury concentrations and pools in two adjacent coniferous and deciduous forests. J. Plant Nut. Soil Sci. 175 (1), 68–77.

Obrist, D., Pokharel, A.K., Moore, C., 2014. Vertical profile measurements of soil air suggest immobilization of gaseous elemental mercury in mineral soil. Environ. Sci. Technol. 48 (4), 2242–2252.

Peña-Rodríguez, S., Pontevedra-Pombal, X., Gayoso, E.G.-R., Moretto, A., Mansilla, R., Cutillas-Barreiro, L., Arias-Estevez, M., Novoa-Munoz, J.C., 2014. Mercury distribution in a toposequence of sub-Antarctic forest soils of Tierra del Fuego (Argentina) as consequence of the prevailing soil processes. Geoderma 232–234, 130–140.

Pokharel, A.K., Obrist, D., 2011. Fate of mercury in tree litter during decomposition. Biogeosci 8, 2593–2627.

Sandilyan, S., Kathiresan, K., 2012. Mangrove conservation: a global perspective. Biodivers. Conserv. 21, 3523–3542.

Shanley, J.B., Mast, M.A., Campbell, D.H., Aiken, G.R., Krabbenhoft, D.P., Hunt, R.J., Walker, J.F., Schuster, P.F., Chalmers, A., Aulenbach, B.T., Peters, N.E., Marvin-DiPasquale, M., Clow, D.W., Shafer, M.M., 2008. Comparison of total mercury and methylmercury cycling at five sites using the small watershed approach. Environ. Pollut. 154 (1), 143–154.

Sherman, L.S., Blum, J.D., 2013. Mercury stable isotopes in sediments and largemouth bass from Florida lakes, USA. Sci. Total Environ. 448, 163–175.

Sonke, J.E., Schäfer, J., Chmeleff, J., Audry, S., Blanc, G., Dupré, B., 2010. Sedimentary mercury stable isotope records of atmospheric and riverine pollution from two major European heavy metal refineries. Chem. Geol. 279, 90–100.

St Louis, V.L., Rudd, J.W.M., Kelly, C.A., Beaty, K.G., Bloom, N.S., Flett, R.J., 1994. Importance of wetlands as sources of methylmercury boreal forest ecosystem. Can. J. Fish. Aqua. Sci. 51, 1065–1076.

Strode, S., Jaegle, L., Selin, N.E., 2009. Impact of mercury emissions from historic gold and silver mining: global modeling. Atmos. Environ. 43, 2012–2017.

Štrok, M., Baya, P.A., Hintelmann, H., 2015. The mercury isotope composition of Arctic coastal seawater. C. R. Geoscience 347, 368–376.

Sun, R.Y., Streets, D.G., Horowitz, H.M., Amos, H.M., Liu, G., Perrot, V., Toutain, J.P., Hintelmann, H., Sunderland, E.M., Sonke, J.E., 2016. Historical (1850–2010) mercury stable isotope inventory from anthropogenic sources to the atmosphere. Elementa. Sci. Anthrop. 4, 000091.

Sun, L., Lu, B., Yuan, D., Hao, W., Zheng, Y., 2017. Variations in the isotopic composition of stable mercury isotopes in typical mangrove plants of the Jiulong Estuary, SE China. Environ. Sci. Pollut. Res. 24, 1459–1468.
USEPA, 2002. Method 1631, Revision E: Mercury in Water by Oxidation, Purge and Trap, and Cold Vapor Atomic Fluorescence Spectrometry. USEPA, WA.
Vannucci, M., 2001. What is so special about mangrove? Braz. J. Biol. 61, 599–603.
Wang, X., Luo, J., Yin, R., Yuan, W., Lin, C.J., Sommar, J., Feng, X., Wang, H., Lin, C., 2017. Using mercury isotopes to understand mercury accumulation in the Montane Forest floor of the Eastern Tibetan Plateau. Environ. Sci. Technol. 51 (2), 801–809.
Wang, X., Yuan, W., Lu, Z., Lin, C.J., Yin, R., Li, F., Feng, X., 2019. Effects of precipitation on mercury accumulation on subtropical montane forest floor: implications on climate forcing. J. Geophys. Res. Biogeosci. 124, 1–14.
Washburn, S.J., Blum, J.D., Demers, J.D., Kurz, A.Y., Landis, R.C., 2017. Isotopic characterization of mercury downstream of historic industrial contamination in the South River, Virginia. Environ. Sci. Technol. 51, 10965–10973.
Wiederhold, J.G., Cramer, C.J., Daniel, K., Infante, I., Bourdon, B., Kretzschmar, R., 2010. Equilibrium mercury isotope fractionation between dissolved Hg(II) species and thiol-bound Hg. Environ. Sci. Technol. 44, 4191–4197.
Woerndle, G., Tsui, M.T.K., Sebestyen, S., Blum, J.D., Nie, X., Kolka, R.K., 2018. New insights on ecosystem mercury cycling revealed by stable isotopes of mercury in water flowing from a headwater peatland catchment. Environ. Sci. Technol. 52 (4), 1854–1861.
Yin, R., Feng, X., Li, Z., Zhang, Q., Bi, X., Li, G., Liu, J., Zhu, J., Wang, J., 2012. Metallogeny and environmental impact of Hg in Zn deposits in China. Appl. Geochem. 27, 151–160.
Yin, R., Feng, X., Meng, B., 2013. Stable mercury isotope variation in Rice Plants (*Oryza sativa* L.) from the Wanshan Mercury Mining District, SW China. Environ. Sci. Technol. 47, 2238–2245.
Yin, R., Feng, X., Chen, B., Zhang, J., Wang, W., Li, X., 2015. Identifying the sources and processes of mercury in subtropical estuarine and ocean sediments using Hg isotopic composition. Environ. Sci. Technol. 49, 1347–1355.
Yin, R., Feng, X., Hurley, J.P., Krabbenhoft, D.P., Lepak, R.F., Hu, R., Zhang, Q., Li, Z., Bi, X., 2016. Mercury isotopes as proxies to identify sources and environmental impacts of mercury in sphalerites. Sci. Rep. 6, 18686.
Yin, R., Guo, Z., Hu, L., Liu, W., Hurley, J.P., Lepak, R.F., Lin, T., Feng, X., Li, X., 2018. Mercury inputs to Chinese marginal seas: impact of industrialization and development of China. J. Geophys. Res. Oceans 123 (8), 5599–5611.
Yoon, J., Cao, X., Zhou, Q., Ma, L.Q., 2006. Accumulation of Pb, Cu and Zn in native plants growing on a contaminated Florida site. Sci. Total Environ. 368, 456–464.
Yu, B., Fu, X., Yin, R., Zhang, H., Wang, X., Lin, C.J., Wu, C., Zhang, Y., He, N., Fu, P., Wang, Z., Shang, L., Sommar, J., Sonke, J.E., Maurice, L., Guinot, B., Feng, X., 2016. Isotopic composition of atmospheric mercury in China: new evidence for sources and transformation processes in air and in vegetation. Environ. Sci. Technol. 50, 9262–9269.
Zhang, H., Yin, R., Feng, X., Sommar, J., Anderson, C.W.N., Sapkota, A., Fu, X., Larssen, T., 2013. Atmospheric mercury inputs in montane soils increase with elevation: evidence from mercury isotope signatures. Sci. Rep. 3, 3322.
Zheng, W., Hintelmann, H., 2009. Mercury isotope fractionation during photoreduction in natural water is controlled by its Hg/DOC ratio. Geochim. Cosmochim. Acta 73, 6704–6715.
Zheng, W., Hintelmann, H., 2010a. Isotope fractionation of mercury during its photochemical reduction by low-molecular-weight organic compounds. J. Phys. Chem. A 114, 4246–4253.
Zheng, W., Hintelmann, H., 2010b. Nuclear field shift effect in isotope fractionation of mercury during abiotic reduction in the absence of light. J. Phys. Chem. A 114, 4238–4245.
Zheng, W., Obrist, D., Weis, D., Bergquist, B.A., 2016. Mercury isotope composition across North American forests. Glob. Biogeochem. Cycles 30, 1475–1492.
Zheng, W., Demers, J., Lu, X., Bergquist, B.A., Anbar, A.D., Blum, J.D., Gu, B., 2019. Mercury stable isotope fractionation during abiotic dark oxidation in the presence of thiols and natural organic matter. Environ. Sci. Technol. https://doi.org/10.1021/acs.est.8b05047.